Journal of Hydrology 608 (2022) 127683

Contents lists available at ScienceDirect

Journal of Hydrology

journal homepage: www.elsevier.com/locate/jhydrol

Research papers

# Development of a stochastic hydrological modeling system for improving ensemble streamflow prediction

Yangshuo Shen [a,b], Shuo Wang [b,c,*], Boen Zhang [b], Jinxin Zhu [d]

[a] School of Economics and Management, North China Electric Power University, Beijing, China
[b] Department of Land Surveying and Geo-Informatics, The Hong Kong Polytechnic University, Hong Kong, China
[c] Shenzhen Research Institute, The Hong Kong Polytechnic University, Shenzhen, China
[d] School of Geography and Planning, Sun Yat-Sen University, Guangzhou, China

A R T I C L E I N F O

This manuscript was handled by Emmanouil Anagnostou, Editor-in-Chief, with the assistance of Yiwen Mei, Associate Editor

*Keywords:*
Hydrological prediction
Streamflow
Uncertainty
Parameter sensitivity

A B S T R A C T

Streamflow prediction plays a crucial role in water resources systems planning and the mitigation of hydrological extremes such as floods and droughts. Since a variety of uncertainties exist in streamflow prediction, it is necessary to enhance our efforts to robustly address uncertainties and their interactions for improving the reliability of streamflow prediction. This paper presents a stochastic hydrological modeling system (SHMS) for improving daily streamflow prediction by explicitly addressing uncertainties in error and model parameters as well as in forcing data and model outputs. Specifically, the SHMS merges the strengths of the ensemble Kalman filter and the particle filter algorithms for improving the effectiveness and robustness of daily streamflow assimilation. Factorial analysis of variance and variance-based global sensitivity analysis are performed to reveal parameter interactions affecting predictive performance and temporal dynamics of parameter sensitivities, maximizing the accuracy of streamflow prediction. The SHMS has been applied to the Guadalupe River basin located in Texas of the United States to demonstrate feasibility and applicability. Our findings indicate that the SHMS improves upon the well-known ensemble Kalman filter for sequential estimation of hydrological model parameters through a more rapid and accurate convergence of model parameters in streamflow simulation. The SHMS also demonstrates a higher level of skill in streamflow prediction compared to the conditional vine copula model. The proposed SHMS can be applied straightforwardly to other river basins for probabilistic hydrological prediction.

## 1. Introduction

Hydrological models have been widely used to advance our understanding of the hydrological cycle in a changing environment. As models are conceptual representations of spatially and temporally varying hydrological processes, uncertainty is inevitable in predicting the behavior of catchments. Uncertainty arises from various sources, including the errors in model structures and parameters, boundary and initial conditions, and hydrometeorological forcing (Ajami et al., 2007; Kavetski et al., 2011; Mockler et al., 2016). Thus, uncertainty assessment plays a crucial role in providing reliable hydrological prediction for sound water resources planning and management.

Uncertainty quantification techniques have been extensively used to explicitly address uncertainties in hydrological prediction (Vrugt et al., 2005; Moradkhani et al., 2005; DeChant and Moradkhani, 2012; Khan and Valeo, 2016; Wang et al., 2018; Huang and Qin, 2018; Abbaszadeh et al., 2019; Ghaith and Li, 2020; Gou et al., 2020; Tran et al., 2020; Ghaith et al., 2021). Over the past decade, the ensemble Kalman filter (EnKF), which is a data assimilation method introduced by Evensen (1994), has been widely used for diagnostic evaluation and uncertainty quantification of hydrological models (Cammalleri and Ciraolo, 2012; Thiboult and Anctil, 2015; Liu et al., 2016; Pathiraja et al., 2016; Zhang et al., 2017; Zou et al., 2017; Tran and Kim, 2021). Previous studies have demonstrated that hydrological data assimilating using the EnKF is able to tackle uncertainties in model parameters, inputs and outputs. As an alternative to the EnKF, the particle filter (PF) technique has been receiving increasing attention in recent years due to its capability to properly estimate the state of nonlinear and non-Gaussian systems (Moradkhani et al., 2012; Vrugt et al., 2013; Wang et al., 2017; Abbaszadeh et al., 2018). Compared with the EnKF, the PF removes the

* Corresponding author at: Department of Land Surveying and Geo-Informatics, The Hong Kong Polytechnic University, Hong Kong, China.
*E-mail address:* shuo.s.wang@polyu.edu.hk (S. Wang).

https://doi.org/10.1016/j.jhydrol.2022.127683
Received 12 September 2021; Received in revised form 15 January 2022; Accepted 27 February 2022
Available online 3 March 2022

Gaussian assumption of the EnKF that often fails to hold for nonlinear systems. However, the PF may suffer from the issue of filter degeneracy where only a few particles have a significant weight while all the others have small weights, which deteriorates the performance of the PF. As a result, a large number of particles are often required to resolve the degeneracy problem, but the ensemble size increases exponentially with the number of state variables, making the PF impractical for high-dimensional models.

Great efforts have been made to the advances in data assimilation techniques over the past decade. Nevertheless, little attention has been paid to the assessment and identification of error parameters and their interactions that have a significant influence on the performance of data assimilation systems. To address uncertainties in model inputs and outputs through data assimilation, an ensemble of model parameters and state variables can be generated through stochastic perturbations of forcing data and observations. The specification of perturbation parameters (i.e. error parameters) is thus the key feature of data assimilation schemes, which plays a crucial role in improving model performance. Since error parameters interact with each other and their interactions have a considerable influence on the behavior of nonlinear dynamic systems, failure to address potential interactions among error parameters can significantly degrade the performance of data assimilation systems. It is thus necessary to identify the best settings of error parameters through examining the contributions of error parameters and their interactions to the performance of data assimilation algorithms. In addition to the assessment of error parameters influencing data assimilation, sensitivities and interactions of model parameters should also be investigated to improve our understanding of dominant model components and their joint behavior.

In this work, we develop a stochastic hydrological modeling system (SHMS) based on sequential data assimilation for improving daily streamflow prediction under uncertainty. Error parameters and their interactions will be examined to identify the best settings of the data assimilation system. Model parameter sensitivities and their temporal dynamics will also be revealed to advance our understanding of the dominant hydrological processes that contribute to the catchment response under time-varying hydroclimatic characteristics. Both synthetic and real data assimilation experiments will be carried out to demonstrate applicability of the proposed methodology in the Guadalupe River basin, Texas. The proposed SHMS will also be compared against the well-known ensemble Kalman filter and the conditional vine copula model to demonstrate superiority.

This paper is organized as follows. Section 2 introduces the proposed methodology for improving daily streamflow prediction. Section 3 provides details on the design and setup of data assimilation experiments. Section 4 presents an in-depth analysis and discussion based on model results and comparison. Finally, conclusions are drawn in Section 5.

## 2. Methodology

### 2.1. Sequential data assimilation algorithms

The basic idea of data assimilation is to produce the best possible estimate of the state of a system through combining different sources of information. These sources include observations and models that inevitably contain errors. The EnKF is a sophisticated data assimilation technique that makes use of Monte Carlo integration methods to approximate the error covariance matrix through a stochastic ensemble of model realizations (Evensen, 2003). The EnKF is particularly useful for nonlinear dynamic models, and can thus be used for the recursive estimation of hydrological model states and parameters. By using the EnKF, the ensemble of model states is integrated forward in time to predict error statistics, and the model forecast can be made as follows:.

$$x^-_{i,t+1} = f\left(x^+_{i,t}, u_{i,t+1}, \theta^-_{i,t+1}\right) + \varepsilon_{i,t+1}, \tag{1}$$

where $x^+_{i,t}$ represent posterior model states at the previous time step, $x^-_{i,t+1}$ represent the predicted model states at the current time step, $f$ represents the hydrological model with model inputs $\mathbf{u}_{i,t+1}$ and parameters $\boldsymbol{\theta}_{i,t+1}$, $\boldsymbol{\varepsilon}_{i,t+1}$ represent model errors, and $i$ and $t$ denote the ensemble number and the time step, respectively. As for the recursive parameter estimation using the EnKF, it is assumed that model parameters are perturbed by a small random noise:.

$$\theta^-_{i,t+1} = \theta^+_{i,t} + \tau S(\theta^-_{i,t}), \tag{2}$$

where $\tau$ is a small tuning parameter of 0.01, and $S(\theta^-_{i,t})$ is the standard deviation of the prior parameter distribution at the previous time step (DeChant and Moradkhani, 2012).

The ensemble members of model states and parameters can then be updated as follows:.

$$x^+_{i,t+1} = x^-_{i,t+1} + K^x_{t+1}\left(y_{t+1} - Hx^-_{i,t+1}\right), \tag{3}$$

$$\theta^+_{i,t+1} = \theta^-_{i,t+1} + K^\theta_{t+1}\left[y_{t+1} - Hx^-_{i,t+1}\right], \tag{4}$$

where $\mathbf{y}_{t+1}$ is the observation vector, $H$ is the observation operator that converts model states to observation space, and $\mathbf{K}_{t+1}$ is the Kalman gain matrix that can be written by:.

$$\mathrm{K}^x_{t+1} = \mathrm{P}^x_{t+1}\mathrm{H}^\mathrm{T}_{t+1}\left(\mathrm{H}_{t+1}\mathrm{P}^x_{t+1}\mathrm{H}^\mathrm{T}_{t+1} + \mathrm{R}_{t+1}\right)^{-1}, \tag{5}$$

$$\mathrm{K}^\theta_{t+1} = \mathrm{P}^\theta_{t+1}\mathrm{H}^\mathrm{T}_{t+1}\left(\mathrm{H}_{t+1}\mathrm{P}^\theta_{t+1}\mathrm{H}^\mathrm{T}_{t+1} + \mathrm{R}_{t+1}\right)^{-1}. \tag{6}$$

where $\mathbf{P}_{t+1}$ is the forecast error covariance, $\mathbf{R}_{t+1}$ is the observation error covariance, and superscript T denotes the matrix transpose.

The PF is a promising alternative to the EnKF, which can be used to derive the posterior distributions of model states by a set of weighted particles. The evolving posterior state distribution can be derived by:.

$$p(\mathrm{x}_{t+1}|\mathrm{y}_{t+1}) = \frac{L(\mathrm{y}_{i,t+1}|\mathrm{x}_{i,t+1})p(\mathrm{x}_{t+1}|\mathrm{y}_t)}{p(\mathrm{y}_{t+1}|\mathrm{y}_t)}, \tag{7}$$

where $p\left(\mathrm{x}_{t+1}, |\mathrm{y}_t\right)$ is the prior state distribution, $p\left(\mathrm{y}_{t+1}, |\mathrm{y}_t\right)$ is a normalization constant, and $L\left(\mathrm{y}_{i,t+1}|\mathrm{x}_{i,t+1}\right)$ is the likelihood function that can be defined as follows:.

$$L(\mathrm{y}_{i,t+1}|\mathrm{x}_{i,t+1}) = \frac{1}{(2\pi)^{m/2}|\mathrm{R}|^{1/2}} exp\left(-\frac{1}{2}(\mathrm{y}_{i,t+1} - \mathrm{H}_x\mathrm{x}_{i,t+1})^T\mathrm{R}^{-1}(\mathrm{y}_{i,t+1} - \mathrm{H}_x\mathrm{x}_{i,t+1})\right). \tag{8}$$

where $\mathbf{R}$ is the observation error covariance matrix, $m$ denotes the length of the observation vector $\mathbf{y}_{i,t+1}$, and $|\bullet|$ denotes the determinant operator.

To address nonlinear and non-Gaussian problems, the sequential Monte Carlo (SMC) method can be used to approximate the posterior state distribution (Doucet et al., 2001):.

$$p(\mathrm{x}_{t+1}, |\mathrm{y}_{t+1}) \approx \sum_{i=1}^{N} \mathrm{w}_{i,t+1}\delta(\mathrm{x}_{t+1} - \mathrm{x}_{i,t+1}), \tag{9}$$

where $\mathbf{y}_{t+1}$ is the observed value at time $t+1$, $\delta(\cdot)$ denotes the Dirac delta function (Gordon et al., 1993), $N$ is the number of particles, and $\mathrm{w}^{+}_{i,t+1}$ is the normalized importance weight for particle $i$ at time $t+1$. Since the posterior density is unknown and difficult to sample directly from$p(\mathrm{x}_{t+1}, |\mathrm{y}_{t+1})$, the particles are usually generated from a known importance density, denoted by$q(\mathrm{x}_{t+1}, |\mathrm{y}_{t+1})$. The unnormalized importance weights of particles can be updated in a recursive form as follows:.

$$\widetilde{w}_{i,t+1} = w_{i,t}\frac{f(x_{i,t+1}|x_{i,t})L(y_{t+1}|x_{i,t+1})}{q(x_{i,t+1}|x_{i,t}, y_{t+1})}, \tag{10}$$

where $f(\mathrm{x}_{i,t+1}|\mathrm{x}_{i,t})L(\mathrm{y}_{t+1}|\mathrm{x}_{i,t+1})/q(\mathrm{x}_{i,t+1}|\mathrm{x}_{i,t}, \mathrm{y}_{t+1})$ is the incremental importance weights (Doucet et al., 2001), $f(\mathrm{x}_{i,t+1}|\mathrm{x}_{i,t})$ is the transition probability density of model states (model operator), and $L(\mathrm{y}_{t+1}|\mathrm{x}_{i,t+1})$ is the likelihood function which is the probability density of observations given state variables (Vrugt et al., 2013). The normalized importance weights of particles can then be calculated by:.

$$w_{i,t+1} = \frac{\widetilde{w}_{i,t+1}}{\sum_{i=1}^{N}\widetilde{w}_{i,t+1}}. \tag{11}$$

The PF algorithm generates a weighted sample of model realizations by updating the particle weights sequentially. Most particles often carry negligible weights after a few iterations, resulting in severe particle degeneracy. The sampling importance resampling (SIR) algorithm can thus be used to address the problem of particle degeneracy (Gilks and Berzuini, 2001; Liu and Chen, 1998). In the SIR algorithm, the update of particles is followed by a resampling step at each time step and all weights become equal after resampling. The resampling step within the PF removes particles with small importance weights and then replaces them by particles with large weights, which is useful to deal with the degeneracy problem.

### 2.2. Stochastic hydrological modeling system

As introduced above, the EnKF and PF algorithms approximate the probability density function (PDF) of the state variable in different ways. The EnKF uses the observed values of state variables to update the forecasted states of each ensemble member, and approximates the state PDF by a set of equally weighted ensemble members. In comparison, the PF does not use a state analysis step; instead, the PF constructs the state PDF by calculating the likelihood (the weight of each particle) which measures in a probabilistic sense the distance between the observed and forecasted state variables. As a result, the PF requires a resampling step to rejuvenate the ensemble since the forecasted states of particles may be systematically biased. From a theoretical point of view, the EnKF estimates the posterior distribution of a state variable at the current observation. In comparison, the PF infers the posterior distribution of the entire state trajectory, which imposes much stronger constraints on the resampling step of a PF as any resampling of the states must be statistically adequate. In other words, the EnKF can simply reset the states close to the measured states; however, this cannot be achieved by a PF because the resampled state would create a state trajectory that is statistically impossible given the model operator and model error. Thus, a stochastic hydrological modeling system (SHMS) is proposed to merge the strengths of the EnKF and PF algorithms for improving the effectiveness of hydrological prediction through data assimilation. The steps to implement the SHMS are shown in Fig. 1.

In the SHMS, the ensemble of model trajectories is produced by stochastically perturbing the precipitation and potential evapotranspiration data as well as streamflow observations, and these perturbations

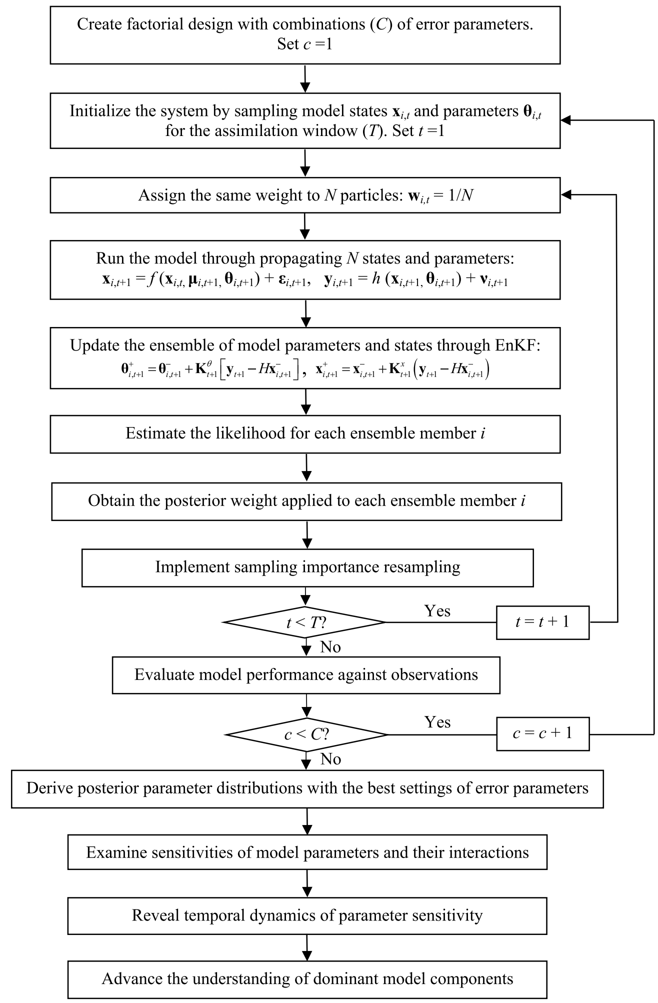


**Fig. 1.** Flowchart of the stochastic hydrological modeling system.

account for uncertainties in model inputs and outputs. As a result, the proper specification of error parameters (i.e. magnitude of perturbations) plays a crucial role in the assimilation accuracy. Factorial ANOVA is an effective statistical technique for examining the effects of independent variables and their interactions on dependent variables through experimental design and data analysis (Montgomery and Runger, 2013). Thus, factorial ANOVA is used in this study to identify the best settings of error parameters with each having specified scenarios through investigating their contributions to model performance, including the precipitation error, the potential evapotranspiration error, and the observation error. The factorial ANOVA model can be expressed as:.

$$y_{ijkl} = \mu + \tau_i + \beta_j + \gamma_k + (\tau\beta)_{ij} + (\tau\gamma)_{ik} + (\beta\gamma)_{jk} + (\tau\beta\gamma)_{ijk} + \varepsilon_{ijkl} \begin{cases} i = 1, 2, \ldots a \\ j = 1, 2, \ldots b \\ k = 1, 2, \ldots c \\ l = 1, 2, \ldots n \end{cases}. \tag{12}$$

where $\mu$ is the overall mean effect, $\boldsymbol{\tau}_i$ is the effect of the $i$th scenario of precipitation error $A$, $\boldsymbol{\beta}_i$ is the effect of the $j$th scenario of potential evapotranspiration error $B$, $\boldsymbol{\gamma}_k$ is the effect of the $k$th scenario of observation error $C$, $(\boldsymbol{\tau\beta})_{ij}$ is the effect of the interaction between error parameters $A$ and $B$, $(\boldsymbol{\tau\gamma})_{ik}$ is the effect of the interaction between error parameters $A$ and $C$, $(\boldsymbol{\beta\gamma})_{jk}$ is the effect of the interaction between error parameters $B$ and $C$, $(\boldsymbol{\tau\beta\gamma})_{ijk}$ is the effect of the interaction among error parameters $A$, $B$, and C, and $\boldsymbol{\varepsilon}_{ijkl}$ is the random error component. The factorial ANOVA model contains three main effects, three two-factor interaction effects, a three-factor interaction effect, and an error term.

These effects can be defined as deviations from the overall mean, so$\sum_{i=1}^{a}\tau_i = 0$, $\sum_{j=1}^{b}\beta_i = 0$, $\sum_{k=1}^{c}\gamma_k = 0$, $\sum_{i=1}^{a}(\tau\beta)_{ij} = \sum_{j=1}^{b}(\tau\beta)_{ij} = 0$, $\sum_{i=1}^{a}(\tau\gamma)_{ik} = \sum_{k=1}^{c}(\tau\gamma)_{ik} = 0$, $\sum_{j=1}^{b}(\beta\gamma)_{jk} = \sum_{k=1}^{c}(\beta\gamma)_{jk} = 0$, and $\sum_{i=1}^{a}(\tau\beta\gamma)_{ijk} = \sum_{j=1}^{b}(\tau\beta\gamma)_{ijk} = \sum_{k=1}^{c}(\tau\beta\gamma)_{ijk} = 0$ (Montgomery, 2000).

To examine the contributions of error parameters and their interactions to model performance, the $F$-statistic can be used as follows:.

$$F_A = \frac{SS_A/a-1}{SS_E/abc(n-1)}, F_B = \frac{SS_B/b-1}{SS_E/abc(n-1)}, F_C = \frac{SS_C/c-1}{SS_E/abc(n-1)}, \tag{13}$$

$$F_{AB} = \frac{SS_{AB}/(a-1)(b-1)}{SS_E/abc(n-1)}, F_{AC} = \frac{SS_{AC}/(a-1)(c-1)}{SS_E/abc(n-1)}, F_{BC} = \frac{SS_{BC}/(b-1)(c-1)}{SS_E/abc(n-1)}, \tag{14}$$

$$F_{ABC} = \frac{SS_{ABC}/(a-1)(b-1)(c-1)}{SS_E/abc(n-1)}. \tag{15}$$

where $SS_A$, $SS_B$, $SS_C$, $SS_{AB}$, $SS_{AC}$, $SS_{BC}$, $SS_{ABC}$, and $SS_E$ are the sum of squares for error parameters $A$, $B$, $C$ and the $A\times B$, $A\times C$, $B\times C$, $A\times B\times C$ interactions as well as the random error component, respectively; $SS_T$ represents the total sum of squares. These statistics are useful for decomposing the total variance into its contributing components, revealing the statistical significance of investigated parameters affecting model performance (Wu and Hamada, 2009). The best settings of error parameters can be identified with maximized performance accordingly.

In addition to factorial ANOVA used to examine the influence of error parameters on model performance, variance-based global sensitivity analysis is also performed in this study to quantify the importance of model parameters. The global sensitivity analysis uses the variance decomposition technique to attribute the total variance in the model output to individual parameters and their interactions. The first- and total-order sensitivity indices are used to reveal the effects of a single parameter and its interactions with other parameters, respectively. These sensitivity indices are calculated using numerical integration with a sample size of 3,000 in a Monte Carlo framework. Furthermore, time-varying sensitivity analysis is performed to explore the temporal dynamics of parameter sensitivities, which is useful for not only improving our understanding of dominant model components under changing hydroclimatic conditions, but also providing meaningful insights (time-varying parameter sensitivities) into uncertainty propagation in hydrological prediction.

### 2.3. Benchmark approach

To demonstrate the superiority of the proposed SHMS, it is necessary to perform a quantitative comparison with existing approaches. The conditional vine copula model was selected as a comparative benchmark since it has been extensively applied to hydrological prediction by constructing a multivariate conditional distribution of hydroclimatic variables (Manning et al., 2018). The conditional vine copula model graphically decomposes a high-dimensional joint distribution into a cascade of bivariate copulas and univariate margins, thereby allowing for flexible hydrological simulations. Assume that $\boldsymbol{x} = (x_1,\dots, x_{n-1}, x_n)$ signifies $n$ hydroclimate variables that affect the streamflow regimes and $y$ signifies the streamflow observation. The joint PDF between $\boldsymbol{x}$ and $\boldsymbol{y}$ can be expressed as.

$$p(x_1,\dots,x_n,y) = p_1(x_1)\cdot\dots\cdot p_n(x_n)\cdot p_y(y)\cdot c(u_1,\dots,u_n,v_y) \tag{16}$$

where $p$ represents the marginal PDF; $u_i$ and $v$ represent the marginal cumulative probability of $x_i$ and $y$, respectively, $i = 1,\dots, n$; $c$ represents the copula density. Since $c(u_1,\dots, u_n, v_y)$ are inflexible in high dimensions and the high-dimensional copula families are limited, vine copula, also known as pair-copula construction (PCC), has been proposed to graphically represent Equation (16) as vines comprising a nested set of trees with nodes that are joined by edges (Bedford & Cooke, 2002). For example, if two hydroclimate variables $(x_1, x_2)$ are used, the joint density between $(x_1, x_2)$ and observation $y$ can be decomposed through a 3-dimensional vine copula as.

$$p(x_1,x_2,y) = p(x_1)\cdot p(x_2)\cdot p(y)\cdot \quad c(u_1,u_2,\alpha_{1,2})\cdot c(u_1,v,\alpha_{1,y})\cdot c\big(h(u_2,u_1,\alpha_{1,2}),h(v,u_1,\alpha_{1,y}),\alpha_{2,y|1}\big) \tag{17}$$

where $\alpha$ represents the parameter set of bivariate copulas; the $h$-function is the conditional distribution function expressed as.

$$F(x|v) = h(x,v,\alpha) = \frac{\partial C_{x,v}\{F(x),F(v),\alpha\}}{\partial F(v)} \tag{18}$$

Since there are multiple vine copula structures to decompose $p(x_1, x_2, y)$, we use the sequential maximal spanning tree algorithm proposed by Dißmann et al. (2013) along with the Akaike information criterion (AIC) to identify an appropriate structure. When the vine structure is determined, a conditional cumulative distribution function (CDF) of $y$ can be constructed by recursively applying the $h$-function:.

$$P(y|x_1,x_2) = \frac{\partial C_{y,2|1}(P(y|x_1),P(x_2|x_1))}{\partial P(x_2|x_1)} = h[h(v,u_1,\alpha_{1,y}),h(u_2,u_1,\alpha_{1,2}),\alpha_{2,y|1}] \tag{19}$$

Thus, the inverse form of Equation (19) can be used to generate probabilistic hydrologic predictions:.

$$\widehat{y} = f(x_1,x_2,\tau) = P_y^{-1}\left\{h^{-1}\left(h^{-1}\left(\tau|h\left(P_2(x_2)|P_1(x_1),\alpha_{1,2}\right),\alpha_{2,y|1}\right)\left|P_1(x_1),\alpha_{1,y}\right.\right)\right\}, \tau\in(0,1) \tag{20}$$

where $\tau$ represents random probability levels (e.g., $\tau = 0.01, 0.1,\dots, 0.99$); $P$ represents marginal CDFs. To achieve reliable model results, MC simulations were used to generate multiple (e.g., 500) samples of $\tau$ from the uniform distribution $U(0, 1)$, leading to multiple realizations of $y$. The median values of these realizations are obtained as hydrological predictions, and uncertainty intervals can also be derived.

## 3. Experimental setups

### 3.1. Study area

The proposed SHMS was applied to predict daily streamflow in the Guadalupe River basin, Texas. As shown in Fig. 2, the Guadalupe River with a drainage area of about 15,500 km$^2$ originates in Kerr County, and flows into the Guadalupe Estuary with a mean daily discharge of 53 m$^3$/

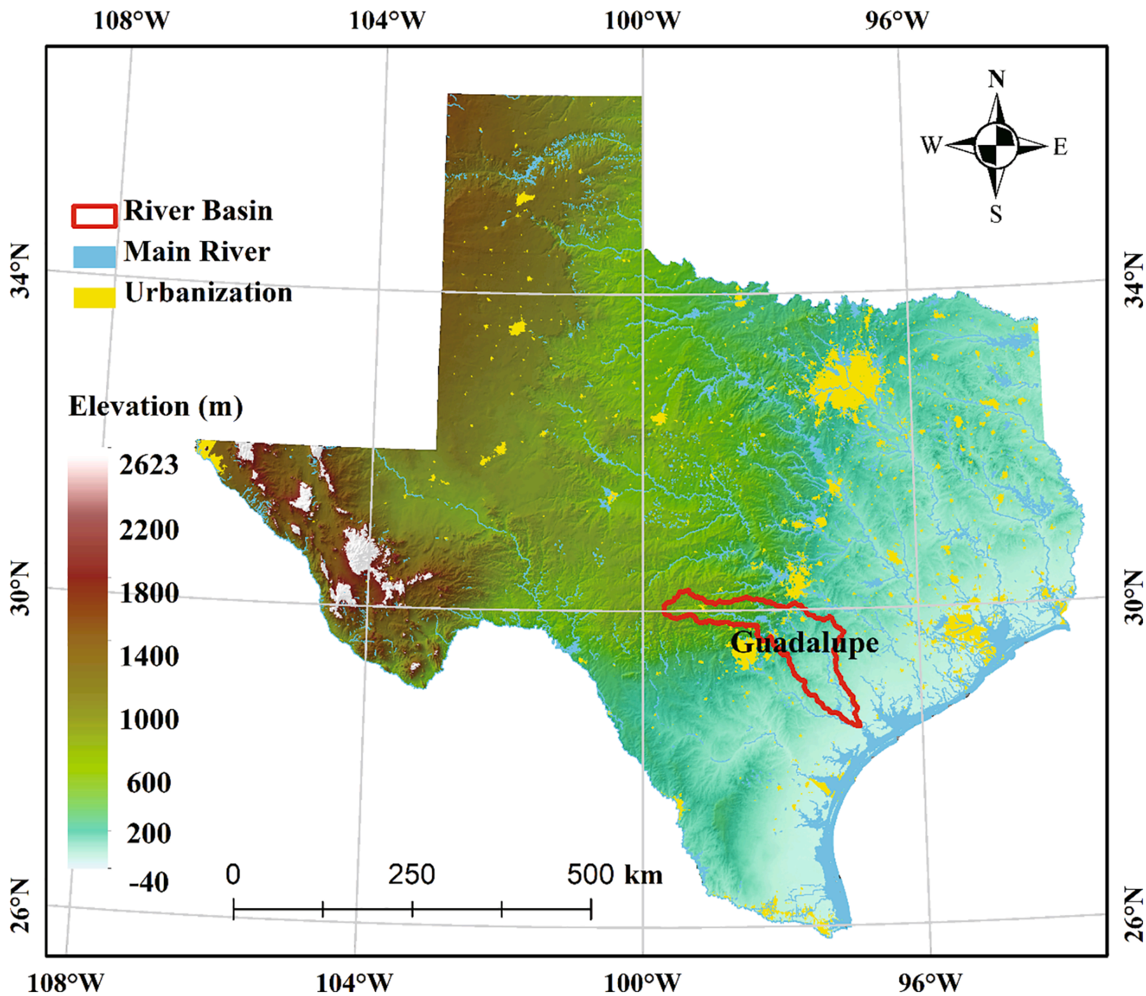


**Fig. 2.** Geographical location and topographic characteristics of the Guadalupe River basin.

s. The Guadalupe River basin is characterized by a significant difference in elevation. The river originates at an elevation of 2,400 feet near its headwaters, while it reaches an elevation as low as 5 feet at the outlet of the basin where the Guadalupe River discharges into the Gulf of Mexico. The Guadalupe River and its tributaries are a vital source of water for a number of populous cities, including Kerrville, New Braunfels, San Marcos, Seguin, Lockhart, Gonzales, Cuero, Luling, and Victoria.

Streamflow conditions in the Guadalupe River basin are mainly influenced by spring discharge, rainfall-runoff processes, evapotranspiration, withdrawals for water supply, reservoir operations, and losses to aquifer recharge (Ockerman and Slattery, 2008). The study area has a subtropical subhumid climate characterized by hot summers and dry winters. Annual precipitation ranges from 770 mm near the headwaters to 1,000 mm near the Gulf of Mexico. The heaviest rainfall tends to occur in spring and early summer. Thus, periods with large or small amounts of rainfall are common, resulting in recurring floods and droughts.

**Table 1**
Initial uncertainty ranges of model parameters and their “true” values.

| Parameter | Description | Range | True value |
|---|---|---|---|
| $C_{max}$ (mm) | Maximum storage capacity of watershed | [10, 1000] | 610 |
| $b_{exp}$ (–) | Degree of spatial variability of soil moisture capacity | [0.0, 10.0] | 2.05 |
| $\beta$ (–) | Factor distributing flow to the quick-flow tank | [0.0, 1.0] | 0.50 |
| $R_s$ (days$^{-1}$) | Residence time of the slow-flow tank | [0.0, 0.2] | 0.15 |
| $R_q$ (days$^{-1}$) | Residence time of the quick-flow tank | [0.1, 1.0] | 0.30 |

### 3.2. Data and model

In this study, the meteorological and hydrological data for the Guadalupe River basin were collected from the Model Parameter Estimation Experiment (MOPEX) dataset (Duan et al., 2006). A total of three years of data from January 1981 to December 1983 were used to assimilate daily streamflow such that the first year was used as a spin-up period to reduce sensitivity to state-value initialization.

Data assimilation experiments were conducted by using the HYMOD which is a widely used rainfall-runoff model for probabilistic hydrological prediction (Bulygina and Gupta, 2011; Sadegh and Vrugt, 2013; Young, 2013; Zhang et al., 2021). In the rainfall-runoff model, the runoff production is characterized as a rainfall excess process, and the runoff is determined according to a probability-distributed storage capacity model that partitions excess rainfall into surface and subsurface storage through a partitioning factor (Moore, 2007). The surface storage is characterized by three quick-flow tanks, and the subsurface storage is represented by a single slow-flow tank. Thus, the generated streamflow is the addition of discharges from slow- and quick-flow tanks.

The model has five parameters, including the maximum soil moisture storage capacity $C_{max}$, the degree of spatial variability in the storage capacity $b_{exp}$, the factor used to distribute flow between the quick- and slow-flow routing $\beta$, the residence time of the slow-flow tank $R_s$, and the residence time of quick-flow tanks $R_q$. The initial ranges of model parameters and their "true" values are given in Table 1. In addition, daily precipitation and potential evapotranspiration are the forcing input data used to drive the model.

### 3.3. Experimental design

Both synthetic and real data assimilation experiments were conducted to demonstrate the proposed methodology. The synthetic experiment was designed to examine the ability of the assimilation system to estimate hydrological model parameters, which has been widely used to validate the performance of data assimilation systems. First, the synthetic experiment with predefined model parameters was carried out to generate the "true" model states and streamflow time series as synthetic observations. Second, the assimilation experiment was conducted based on the generated synthetic streamflow time series such that the convergence of model parameters towards the predefined parameter values can be evaluated. Third, the assimilation experiment with real streamflow data was conducted when the performance of the assimilation system was validated through the synthetic experiment.

To address various sources of uncertainty in data assimilation,

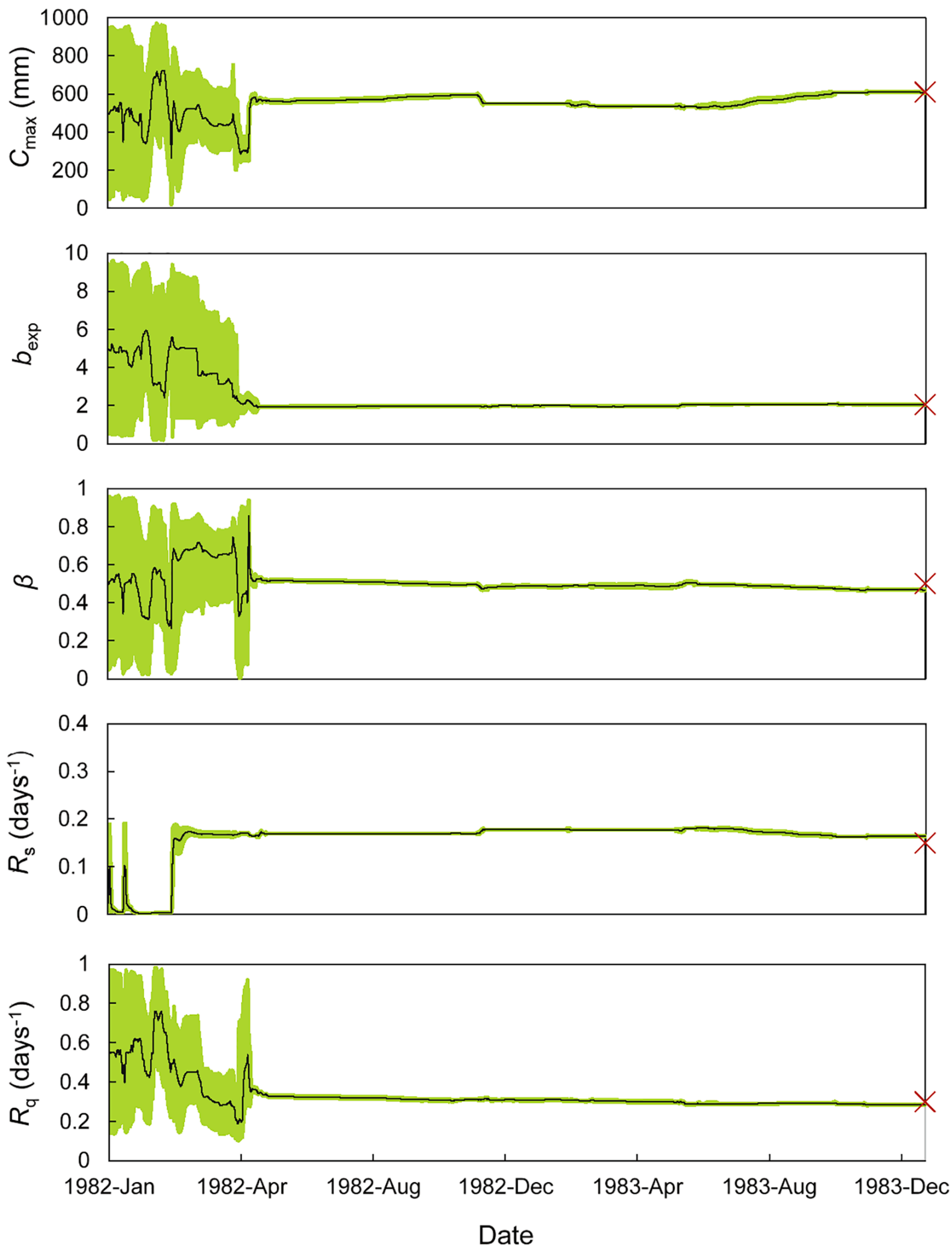


**Fig. 3.** Convergence of model parameters to "true" values. Shaded areas and solid lines represent 90% uncertainty intervals and mean values, respectively. Crosses denote "true" parameter values.

random perturbations were adopted by adding noise (errors) to the precipitation and potential evapotranspiration data and streamflow observations, leading to an ensemble of state variables. As a result, the specification of error parameters is a key feature of assimilation systems, which plays an important role in the performance of hydrological prediction. A statistical hypothesis test was conducted in this study to identify the best settings of error parameters including the precipitation error, the potential evapotranspiration error, and the streamflow observation error. Three scenarios were given on the strength of perturbations, including 10%, 30%, and 50%. A three-way factorial ANOVA was thus performed to explicitly examine the sensitivities of error parameters and their interactions affecting the predictive accuracy, which provided meaningful information for achieving the best performance of hydrological prediction. When the posterior distributions of error parameters were identified through data assimilation, the sensitivities of model parameters and their interactions were then investigated through variance-based global sensitivity analysis, advancing our understanding of dominant hydrological components and their temporal evolution.

## 4. Results and discussion

### 4.1. Evaluation of the SHMS for parameter estimation

A synthetic data assimilation experiment was performed to demonstrate the ability of SHMS to estimate the predefined model parameters. Fig. 3 shows the convergence of model parameters through assimilating streamflow observations. All parameters are identifiable as they rapidly converge to the posterior target distributions, and the estimated mean

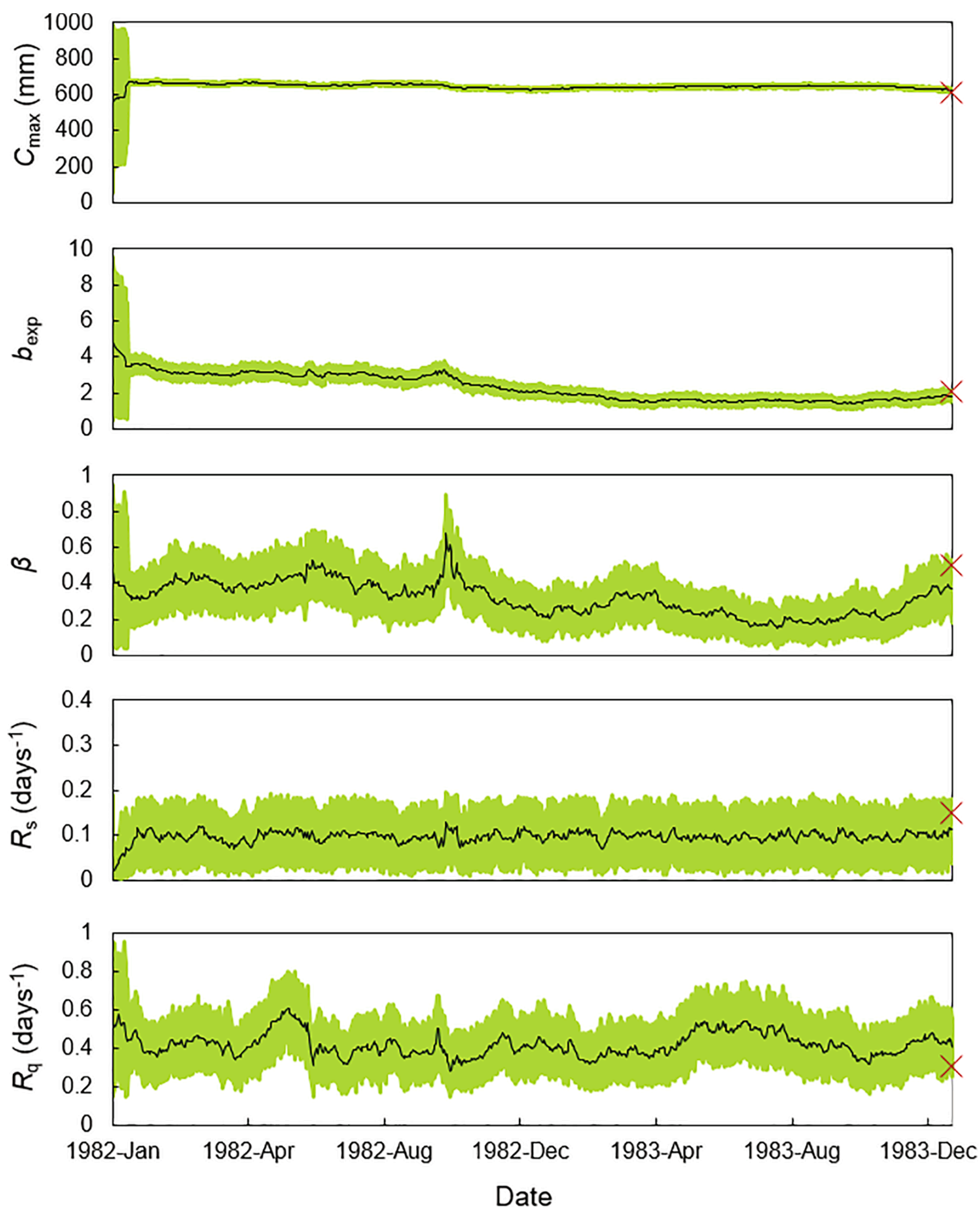


**Fig. 4.** Convergence of model parameters estimated through streamflow assimilation using the ensemble Kalman filter (EnKF) algorithm.

values of all parameters converge toward the “true” values which are predefined as: $C_{\max} = 610$ mm, $b_{\exp} = 2.05$, $\beta = 0.50$, $R_s = 0.15$ days$^{-1}$, and $R_q = 0.30$ days$^{-1}$. It can be seen that the first two parameters $C_{\max}$ and $b_{\exp}$ related to soil moisture storage capacity can be better estimated compared to the others.

As new observations become available, the SHMS recursively correct and update parameter samples. Thus, the uncertainty degree (i.e. difference between maximum and minimum values) of model parameters is relatively high at the early stage of filtering, and diminishes gradually along the assimilation trajectory. Results verify the ability of SHMS to achieve convergence to the target distributions, and can thus be used for uncertainty assessment of hydrological model parameters and predictions. To further demonstrate the advantage of the proposed approach, the data assimilation results obtained from the SHMS are compared against those obtained with the well-known EnKF. Fig. 4 depicts the evolution of model parameters estimated using the EnKF. In comparison, the proposed SHMS largely improves upon the EnKF through the more rapid and accurate convergence of model parameters towards the posterior target distributions with reduced uncertainty, especially for estimating the factor used to distribute flow between the quick- and slow-flow routing ($\beta$), the residence time of the slow-flow tank ($R_s$), and the residence time of quick-flow tanks ($R_q$).

### 4.2. Identification of error and model parameters in streamflow assimilation

When the performance of the SHMS was validated through the synthetic experiment, a real data assimilation experiment was also conducted to predict daily streamflow in the Guadalupe River basin, Texas. A three-way factorial ANOVA was performed to examine the impacts of model and observation error parameters as well as their interactions in streamflow assimilation so as to identify the best settings of the SHMS with maximized performance. Fig. 5 presents the normal probability plot of residuals for checking the normality of the residual distribution in the three-way ANOVA. Since this plot is approximately linear, it verifies that the residuals are normally distributed.

As shown in Table 2, the precipitation error is identified as the most statistically significant parameter according to the $p$-value. Thus, the precipitation error parameter has the largest first-order effect on the predictive accuracy. This indicates that any change in the settings of precipitation error parameter could lead to the largest variation of the root mean square error (RMSE) value. In addition, the potential evapotranspiration and the streamflow observation error parameters as well as their interactions have considerable contributions to model performance. Based on the interaction analysis through factorial

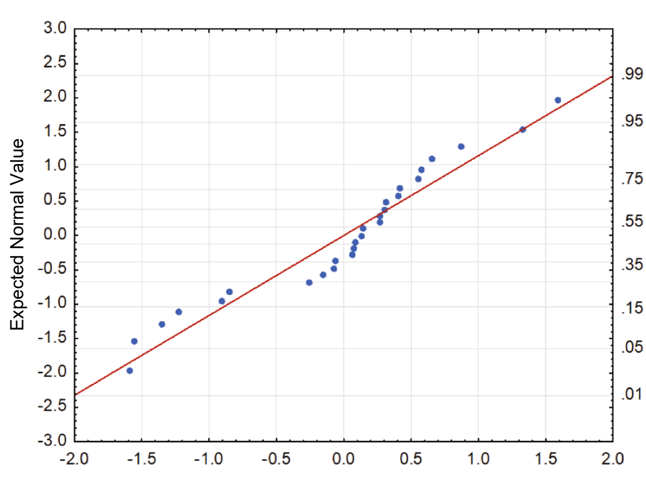


**Fig. 5.** Normal probability plot of raw residuals.

**Table 2**
Three-way factorial ANOVA for error parameters.

| Error parameter | Sum of squares | Degrees of freedom | Mean square | F-value | P-value |
|---|---|---|---|---|---|
| PreError (L) | 10.11 | 1 | 10.11 | 10.27 | 0.005 |
| PreError (Q) | 1.84 | 1 | 1.84 | 1.87 | 0.189 |
| EvaError (L) | 7.95 | 1 | 7.95 | 8.08 | 0.011 |
| EvaError (Q) | 2.56 | 1 | 2.56 | 2.60 | 0.125 |
| ObsError (L) | 4.90 | 1 | 4.90 | 4.98 | 0.039 |
| ObsError (Q) | 0.89 | 1 | 0.89 | 0.91 | 0.354 |
| PreError × EvaError | 1.22 | 1 | 1.23 | 1.25 | 0.279 |
| PreError × ObsError | 4.53 | 1 | 4.53 | 4.60 | 0.046 |
| EvaError × ObsError | 9.95 | 1 | 9.95 | 10.11 | 0.005 |
| Error | 16.73 | 17 | 0.98 | | |
| Total sum of squares | 60.72 | 26 | | | |

Note: PreError, EvaError, and ObsError represent precipitation error, potential evapotranspiration error, and observation error, respectively. (L) and (Q) denote the first- and second-order effects, respectively.

ANOVA, the minimum value of RMSE can be obtained when the settings of precipitation, potential evapotranspiration, and observation error parameters are 50%, 10%, and 50%, respectively. Identification of the best settings of error parameters provides meaningful information for advancing our understanding of the data assimilation system and for maximizing model performance. In previous studies, error parameters were often randomly selected without a systematic assessment, resulting in unreliable conclusions due to the oversimplified settings of error parameters. For instance, a single scenario of error parameters was often used previously to carry out hydrological data assimilation. However, sensitivities of error parameters and their interactions play a crucial role in the performance of data assimilation. It is thus necessary to examine various scenarios of error parameters and to explore potential interactions between error parameters affecting the predictive accuracy, leading to more robust and reliable hydrological prediction with the best parameter settings.

Fig. 6 shows the temporal evolution of model parameters derived through the daily streamflow assimilation using the SHMS with the best settings of error parameters. It is indicated that all parameters are identifiable, and they converge rapidly to the target distributions. The derived posterior parameter distributions vary greatly from the synthetic experiment to the real data experiment due to the assimilation of different streamflow time series. Fig. 7 presents a comparison of simulated and observed daily streamflow time series. The daily streamflow distributions were evaluated using the probabilistic performance measure of “reliability” introduced by Renard et al. (2010) and Breinholt et al. (2012). “Reliability” represents the percentage of observations falling within the uncertainty bounds of simulated streamflow time series, which varies between 0 (lowest reliability) and 1 (highest reliability). In this study, the reliability of streamflow distribution is 0.75 which is acceptable although far from perfect, but the SHMS may underpredict the streamflow regimes. Furthermore, hypothesis testing with a significance level of 0.05 was conducted to measure the significance of the difference between observed and simulated streamflow time series. The $p$-value derived by the hypothesis testing is less than 0.05, which indicates that the accuracy of streamflow prediction is statistically acceptable. This verifies the ability of the SHMS to recursively assimilate streamflow observations, and can thus be used for probabilistic streamflow prediction in the Guadalupe River basin.

### 4.3. Comparison with probabilistic prediction approach

To demonstrate the superiority of the proposed SHMS, the conditional vine copula model was selected as a comparative benchmark. To

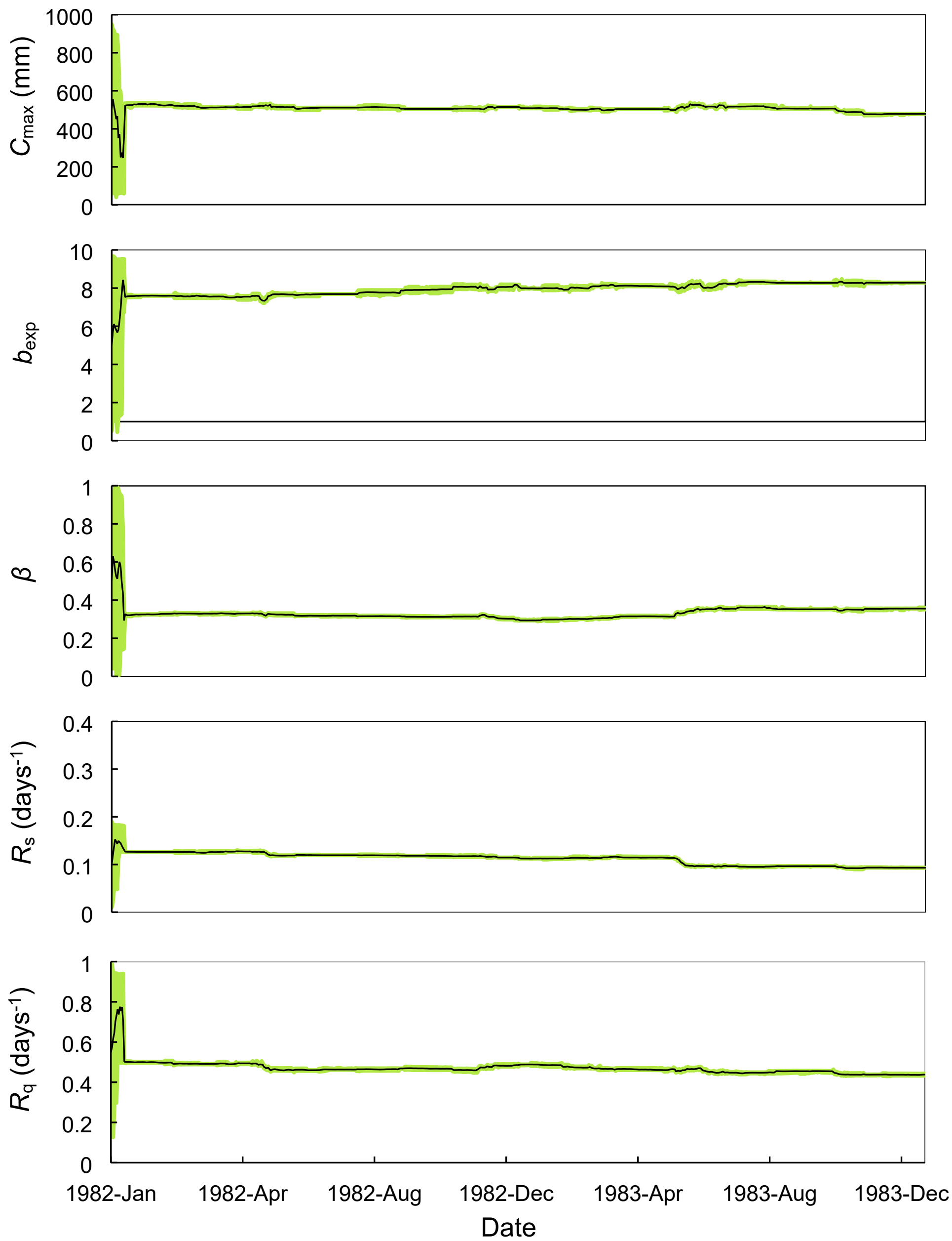


**Fig. 6.** Temporal evolution of model parameters in streamflow assimilation.

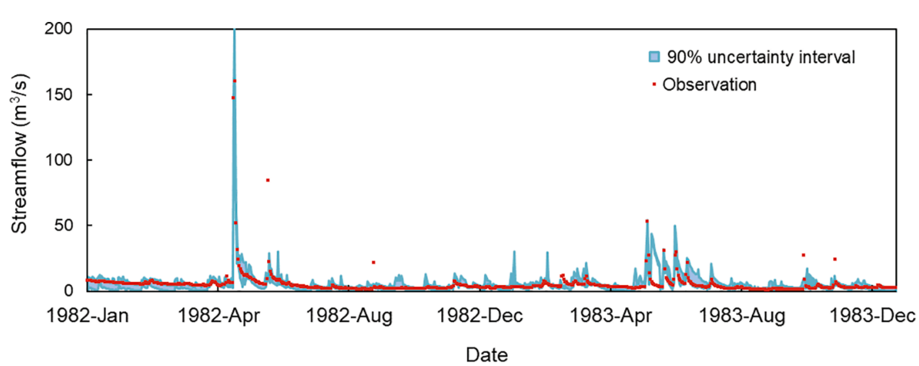


**Fig. 7.** Daily streamflow time series with 90% uncertainty intervals.

**Table 3**
Selection of marginal distributions of hydrological variables using AIC. PET = potential evapotranspiration. AIC = Akaike information criterion.

| Variable | gamma | Weibull | log-normal | Gumbel | GEV | log-logistic | GP | generalized gamma |
|---|---|---|---|---|---|---|---|---|
| Streamflow | 5348 | 5291 | 5001 | 5817 | **0.73** | 4954 | 5134 | 6 |
| Precipitation | 1442 | 1391 | 1357 | 2455 | **−1.47** | 1389 | 1404 | 1359 |
| PET | 5732 | 5666 | 5798 | 5808 | **−2.81** | 5943 | 5530 | 2565 |
| Temperature | 5225 | 5065 | 5355 | 5274 | **1.55** | 5264 | 5401 | 4989 |

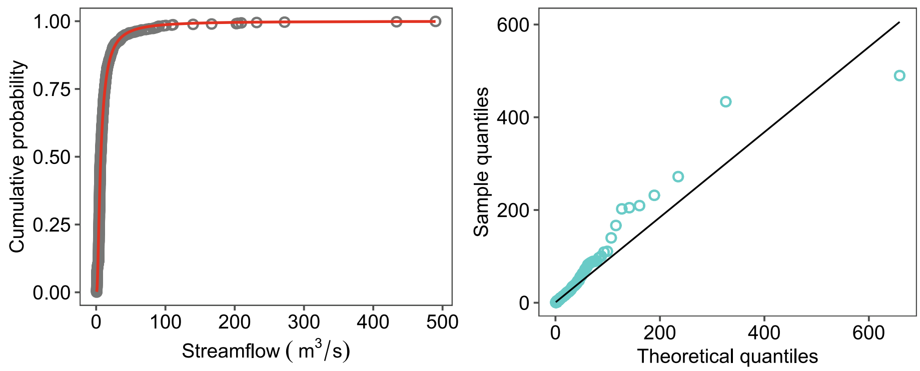


**Fig. 8.** The GEV distribution of daily streamflow over the Guadalupe river basin during 1982–1983. GEV = generalized extreme value.

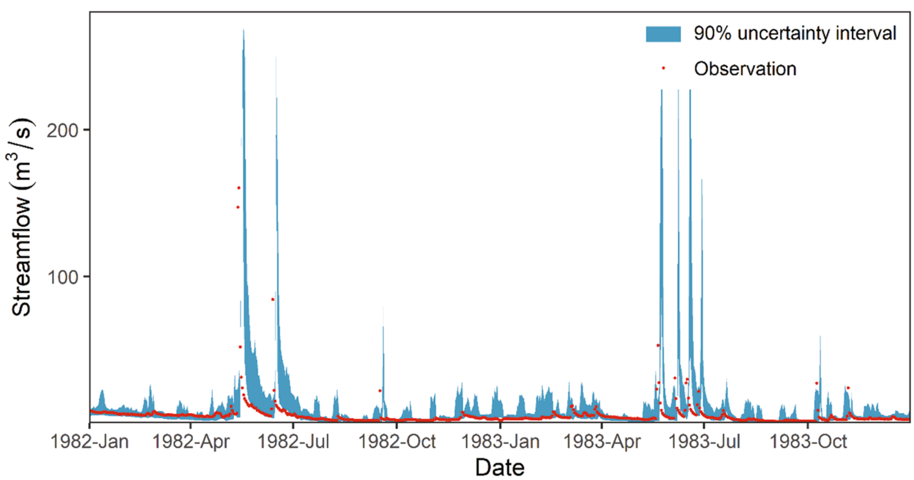


**Fig. 9.** Daily streamflow prediction generated from the conditional vine copula model over the Guadalupe river basin.

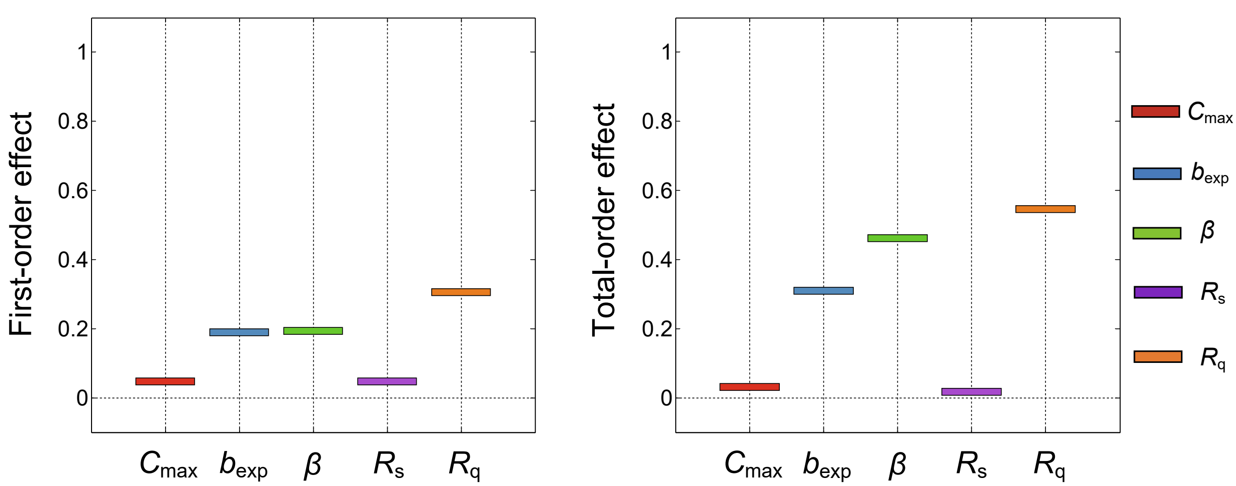


**Fig. 10.** First- and total-order effects of model parameters.

construct a conditional vine copula model, the marginal distributions of hydrological variables (i.e., streamflow, precipitation, potential evapotranspiration, and temperature) were selected from a total of 8 types of probability distributions, including gamma, Weibull, log-normal, Gumbel, generalized extreme value (GEV), log-logistic, generalized Pareto (GP), and generalized gamma.

The marginal distribution of hydrological variables was selected using the Akaike information criterion (AIC) (see Table 3). Results show that the GEV distribution was optimal for all hydrological variables, including streamflow, precipitation, potential evapotranspiration, and temperature. For example, Fig. 8 presents the fitted GEV cumulative distribution function of daily streamflow and the Q-Q plot, indicating that the GEV distribution provides a good representation of daily streamflow. The hydrological variables were transformed to uniform margins on [0, 1] based on their optimal parametric probability distributions and then were used to construct the conditional vine copula model. The one with the lowest AIC value was selected as the optimal vine structure. Fig. 9 presents a comparison of daily streamflow time series generated from the observation and the constructed conditional vine copula model. Results show that the reliability is 0.71, which is lower than 0.75 generated from the proposed SHMS. The SHMS also outperforms the conditional vine copula model in terms of capturing extreme flows. Specifically, the SHMS captures 81% and 83% of high (i.e., higher than the 90th percentile) and low (i.e., lower than the 10th percentile) flows, respectively, whereas the conditional vine copula model captures only 71% and 36% of high and low flows, respectively. This indicates that the proposed SHMS can improve the reliability of daily streamflow simulations by robustly addressing various uncertainties and their interactions.

### 4.4. Sensitivities of model parameters and their interactions

Variance-based global sensitivity analysis was also carried out to examine the sensitivities of model parameters and their interactions. As shown in Fig. 10, the residence time of the quick-flow tank $R_q$ has the largest individual and interaction effects on model performance. This indicates that the simulated daily streamflow is highly sensitive to the variation of the residence time of the quick-flow tank. Thus, the quick-flow tank parameter plays a crucial role in streamflow predictions in the Guadalupe River basin.

In addition, the quick-flow tank parameter is closely correlated with other parameters, and their interactions make a considerable contribution to model performance. In comparison, the residence time of the slow-flow tank $R_s$ and its interactions with other parameters make little contribution to model performance. Results indicate that the surface runoff routing plays a dominant role in minimizing the overall error, while the subsurface runoff process has little influence on streamflow predictions in the Guadalupe River basin. Consequently, sensitivity analysis for model parameters and their interactions is useful for providing meaningful insights into model components dominating the overall accuracy.

As the parameter sensitivity varies over time due to the changing hydrological conditions, the temporal dynamics of parameter sensitivity were examined using the time-varying sensitivity analysis method introduced by Pianosi and Wagener (2016). As shown in Fig. 11, sensitivities of five model parameters vary in response to changes in daily streamflow. The accuracy is highly sensitive to the degree of spatial variability of soil moisture capacity $b_{exp}$ and the residence time of the quick-flow tank $R_q$, especially for the days with heavy rainfall. Our findings reveal that the soil moisture capacity and the surface runoff routing parameters as well as precipitation play a key role in simulating daily streamflow in the dry Guadalupe River basin. In addition, minimizing errors in heavy rainy days would greatly improve the overall accuracy of daily streamflow predictions. Analysis of the temporal dynamics of parameter sensitivity advances our understanding of dominant hydrologic processes that contribute to the catchment response under time-varying hydroclimatic conditions.

## 5. Conclusions

In this study, we proposed a SHMS for improving daily streamflow prediction through sequential data assimilation. The SHMS greatly improves upon the well-known EnKF through the more rapid and accurate convergence of model parameters in streamflow assimilation. Factorial ANOVA was performed to explicitly reveal the impacts of model and observation error parameters as well as their interactions on streamflow assimilation. Variance-based sensitivity analysis was also conducted to examine the sensitivities of hydrological model parameters and their interactions as well as to reveal the temporal dynamics of parameter sensitivity. Such a computational framework is capable of explicitly identifying underlying interactions between error parameters in streamflow assimilation and robustly predicting daily streamflow time series in a probabilistic manner. The proposed framework was also compared with the existing well-known approach used for streamflow prediction.

Both synthetic and real data assimilation experiments were conducted to demonstrate applicability of the proposed methodology in the Guadalupe River basin, Texas. Results obtained from factorial ANOVA reveal that the precipitation error parameter has the largest first-order effect on the assimilation accuracy. Potential evapotranspiration and

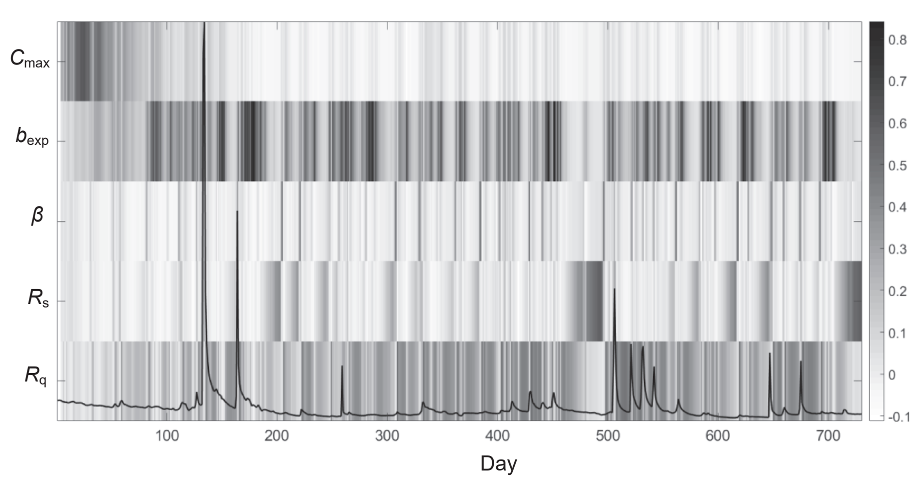


**Fig. 11.** Temporal variation in the sensitivity of model parameters. The black line represents the time series of simulated streamflow. The grayscale represents the time-varying parameter sensitivity (i.e. contribution of each parameter to the total variance of model output).

streamflow observation error parameters as well as their interactions have considerable contributions to model performance. Factorial ANOVA provides insights into model and observation error parameters that affect the performance of the hydrological data assimilation system, maximizing the accuracy of streamflow assimilation. By comparing the time series of observed and simulated daily streamflow using deterministic and probabilistic measures, the results verify the ability of the SHMS to properly assimilate streamflow observations in the Guadalupe River basin. The SHMS also shows better performance than the conditional vine copula model in terms of the reliability of streamflow prediction. On the other hand, the soil moisture capacity and the surface runoff routing parameters as well as precipitation play a crucial role in simulating daily streamflow in the dry Guadalupe River basin. Moreover, sensitivities of model parameters vary over time due to the changing hydroclimatic conditions. The model response is more sensitive to the variation of model parameters for the days with heavy rainfall. Thus, minimizing errors in heavy rainy days would greatly improve the overall accuracy. These findings provide meaningful insights into the dynamics of model components dominating the overall performance.

The SHMS has significant potential for performing hydrological predictions, and will be applied to the physically-based distributed hydrological models for better addressing the spatial heterogeneity of watershed characteristics in future studies. Nevertheless, the computational cost will increase exponentially with the increasing number of hydrological model parameters due to the computationally extensive factorial ANOVA and the variance-based global sensitivity analysis. It is thus necessary to further improve the factorial design and the variance-based sensitivity analysis method for increasing the computational efficiency of hydrological prediction using the SHMS. Moreover, a total of three years of data collected from the MOPEX dataset are used in this study to predict daily streamflow, which may not adequately reflect the hydrological characteristics. The longer time series data is thus desired in future studies to further improve the robustness of hydrological prediction.

## CRediT authorship contribution statement

**Y. Shen:** Methodology, Validation, Formal analysis, Investigation, Writing – original draft. **S. Wang:** Conceptualization, Formal analysis, Writing – review & editing, Supervision, Project administration, Funding acquisition. **B. Zhang:** Validation, Formal analysis, Writing – original draft. **J. Zhu:** Writing – original draft.

## Declaration of Competing Interest

The authors declare that they have no known competing financial interests or personal relationships that could have appeared to influence the work reported in this paper.

## Acknowledgments

This research was supported by the National Natural Science Foundation of China (Grant No. 51809223) and the Hong Kong Research Grants Council Early Career Scheme (Grant No. 25222319). The daily meteorological and hydrological data for the Guadalupe River basin were collected from the U.S. MOPEX dataset.

## References

Abbaszadeh, P., Moradkhani, H., Daescu, D.N., 2019. The quest for model uncertainty quantification: A hybrid ensemble and variational data assimilation framework. Water Resour. Res. 55 (3), 2407–2431.

Abbaszadeh, P., Moradkhani, H., Yan, H., 2018. Enhancing hydrologic data assimilation by evolutionary Particle Filter and Markov Chain Monte Carlo. Adv. Water Resour. 111, 192–204.

Ajami, N.K., Duan, Q., Sorooshian, S., 2007. An integrated hydrologic Bayesian multimodel combination framework: confronting input, parameter, and model structural uncertainty in hydrologic prediction. Water Resour. Res. 43 (1), W01403.

Bedford, T., Cooke, R.M., 2002. Vines – a new graphical model for dependent random variables. Ann. Stat. 30, 1031–1068.

Breinholt, A., Møller, J.K., Madsen, H., Mikkelsen, P.S., 2012. A formal statistical approach to representing uncertainty in rainfall–runoff modelling with focus on residual analysis and probabilistic output evaluation – distinguishing simulation and prediction. J. Hydrol. 472–473, 36–52.

Bulygina, N., Gupta, H., 2011. Correcting the mathematical structure of a hydrological model via Bayesian data assimilation. Water Resour. Res. 47 (5), W05514.

Cammalleri, C., Ciraolo, G., 2012. State and parameter update in a coupled energy/hydrologic balance model using ensemble Kalman filtering. J. Hydrol. 416–417, 171–181.

Dißmann, J., Brechmann, E.C., Czado, C., Kurowicka, D., 2013. Selecting and estimating regular vine copulae and application to financial returns. Comput. Stat. Data Anal. 59, 52–69.

DeChant, C.M., Moradkhani, H., 2012. Examining the effectiveness and robustness of sequential data assimilation methods for quantification of uncertainty in hydrologic forecasting. Water Resour. Res. 48 (4), W04518.

Doucet, A., de Freitas, N., Gordon, N., 2001. Seqential Monte Carlo Methods in Practice. Springer, New York, p. 581.

Duan, Q., et al., 2006. Model Parameter Estimation Experiment (MOPEX): An overview of science strategy and major results from the second and third workshops. J. Hydrol. 320 (1–2), 3–17.

Evensen, G., 1994. Sequential data assimilation with a nonlinear quasi-geostrophic model using Monte Carlo methods to forecast error statistics. J. Geophys. Res.-Oceans 99 (C5), 10143–10162.

Evensen, G., 2003. The Ensemble Kalman Filter: theoretical formulation and practical implementation. Ocean Dynam. 53 (4), 343–367.

Ghaith, M., Li, Z., 2020. Propagation of parameter uncertainty in SWAT: A probabilistic forecasting method based on polynomial chaos expansion and machine learning. J. Hydrol. 586, 124854.

Ghaith, M., Li, Z., Baetz, B.W., 2021. Uncertainty analysis for hydrological models with interdependent parameters: An improved polynomial chaos expansion approach. Water Resour. Res., 57 (8), e2020WR029149.

Gilks, W.R., Berzuini, C., 2001. Following a moving target-Monte Carlo inference for dynamic Bayesian models. J. R. Stat. Soc. Ser. B 63 (1), 127–146.

Gordon, N.J., Salmond, D.J., Smith, A.F.M., 1993. Novel approach to nonlinear/non-Gaussian Bayesian state estimation. IEE Proc. Radar Signal Process. 140 (2), 107–113.

Gou, J., Miao, C., Duan, Q., Tang, Q., Di, Z., Liao, W., Wu, J., Zhou, R., 2020. Sensitivity analysis-based automatic parameter calibration of the VIC model for streamflow simulations over China. Water Resour. Res., 56 (1), e2019WR025968.

Huang, Y., Qin, X.S., 2018. Uncertainty assessment of flood inundation modelling with a 1D/2D random field. J. Hydroinform. 20 (5), 1148–1162.

Kavetski, D., Fenicia, F., Clark, M.P., 2011. Impact of temporal data resolution on parameter inference and model identification in conceptual hydrological modeling: Insights from an experimental catchment. Water Resour. Res. 47 (5), W05501.

Khan, U.T., Valeo, C., 2016. Short-term peak flow rate prediction and flood risk assessment using fuzzy linear regression. J. Environ. Inform. 28 (2), 71–89.

Liu, D., Mishra, A.K., Yu, Z., 2016. Evaluating uncertainties in multi-layer soil moisture estimation with support vector machines and ensemble Kalman filtering. J. Hydrol. 538, 243–255.

Liu, J.S., Chen, R., 1998. Sequential Monte Carlo methods for dynamic systems. J. Am. Stat. Assoc. 93 (443), 1032–1044.

Manning, C., Widmann, M., Bevacqua, E., Van Loon, A.F., Maraun, D., Vrac, M., 2018. Soil moisture drought in Europe: a compound event of precipitation and potential evapotranspiration on multiple time scales. J. Hydrometeorol. 19, 1255–1271.

Mockler, E.M., Chun, K.P., Sapriza-Azuri, G., Bruen, M., Wheater, H.S., 2016. Assessing the relative importance of parameter and forcing uncertainty and their interactions in conceptual hydrological model simulations. Adv. Water Resour. 97, 299–313.

Moradkhani, H., DeChant, C.M., Sorooshian, S., 2012. Evolution of ensemble data assimilation for uncertainty quantification using the particle filter-Markov chain Monte Carlo method. Water Resour. Res. 48 (12), W12520.

Moradkhani, H., Sorooshian, S., Gupta, H.V., Houser, P.R., 2005. Dual state–parameter estimation of hydrological models using ensemble Kalman filter. Adv. Water Resour. 28 (2), 135–147.

Montgomery, D., 2000. Design and Analysis of Experiments, fifth ed. John Wiley & Sons, New York.

Montgomery, D.C., Runger, G.C., 2013. Applied Statistics and Probability for Engineers, sixth ed. John Wiley & Sons, New York.

Moore, R.J., 2007. The PDM rainfall-runoff model. Hydrol. Earth Syst. Sci. 11 (1), 483–499.

Ockerman, D.J., Slattery, R.N., 2008. Streamflow conditions in the Guadalupe River Basin, south-central Texas, water years 1987–2006 — An assessment of streamflow gains and losses and relative contribution of major springs to streamflow: U.S. Geological Survey Scientific Investigations Report 2008–5165, 22 p.

Pathiraja, S., Marshall, L., Sharma, A., Moradkhani, H., 2016. Hydrologic modeling in dynamic catchments: a data assimilation approach. Water Resour. Res. 52 (5), 3350–3372.

Pianosi, F., Wagener, T., 2016. Understanding the time-varying importance of different uncertainty sources in hydrological modelling using global sensitivity analysis. Hydrol. Process. 30, 3991–4003.

Renard, B., Kavetski, D., Kuczera, G., Thyer, M., Franks, S.W., 2010. Understanding predictive uncertainty in hydrologic modeling: the challenge of identifying input and structural errors. Water Resour. Res. 46, W05521.

Sadegh, M., Vrugt, J.A., 2013. Bridging the gap between GLUE and formal statistical approaches: approximate Bayesian computation. Hydrol. Earth Syst. Sci. 17, 4831–4850.

Thiboult, A., Anctil, F., 2015. On the difficulty to optimally implement the Ensemble Kalman filter: an experiment based on many hydrological models and catchments. J. Hydrol. 529, 1147–1160.

Tran, V.N., Dwelle, M.C., Sargsyan, K., Ivanov, V.Y., Kim, J., 2020. A novel modeling framework for computationally efficient and accurate real-time ensemble flood forecasting with uncertainty quantification. Water Resour. Res., 56 (3), e2019WR025727.

Tran, V.N., Kim, J., 2021. A robust surrogate data assimilation approach to real-time forecasting using polynomial chaos expansion. J. Hydrol. 126367.

Vrugt, J.A., Diks, C.G.H., Gupta, H.V., Bouten, W., Verstraten, J.M., 2005. Improved treatment of uncertainty in hydrologic modeling: Combining the strengths of global optimization and data assimilation. Water Resour. Res. 41 (1), W01017.

Vrugt, J.A., ter Braak, C.J.F., Diks, C.G.H., Schoups, G., 2013. Hydrologic data assimilation using particle Markov chain Monte Carlo simulation: Theory, concepts and applications. Adv. Water Resour. 51, 457–478.

Wang, S., Huang, G.H., Baetz, B.W., Ancell, B.C., 2017. Towards robust quantification and reduction of uncertainty in hydrologic predictions: Integration of particle Markov chain Monte Carlo and factorial polynomial chaos expansion. J. Hydrol. 548, 484–497.

Wang, S., Ancell, B.C., Huang, G.H., Baetz, B.W., 2018. Improving robustness of hydrologic ensemble predictions through probabilistic pre- and post-processing in sequential data assimilation. Water Resour. Res. 54, 2129–2151.

Wu, C.F.J., Hamada, M.S., 2009. Experiments: Planning, Analysis, and Optimization. John Wiley & Sons, New Jersey.

Young, P.C., 2013. Hypothetico-inductive data-based mechanistic modeling of hydrological systems. Water Resour. Res. 49 (2), 915–935.

Zhang, B., Wang, S., Wang, Y., 2021. Probabilistic projections of multidimensional flood risks at a convection-permitting scale. Water Resour. Res., 57, e2020WR028582.

Zhang, H., Hendricks Franssen, H.-J., Han, X., Vrugt, J.A., Vereecken, H., 2017. State and parameter estimation of two land surface models using the ensemble Kalman filter and the particle filter. Hydrol. Earth Syst. Sci. 21, 4927–4958.

Zou, L., Zhan, C., Xia, J., Wang, T., Gippel, C.J., 2017. Implementation of evapotranspiration data assimilation with catchment scale distributed hydrological model via an ensemble Kalman Filter. J. Hydrol. 549, 685–702.